

Kinematics Modelling, Optimization and Control of Hybrid Robots

Mahmoud Tarokh^a and Federico Llenar

Department of computer Science, San Diego State University, San Diego, CA 92182-7720, U.S.A.

Keywords: Hybrid Robots, Rolling and Walking Kinematics.

Abstract: The paper develops a unified kinematics modelling, optimization and control for hybrid robots. These robots combine two or more modes of operations, such as a combination of walking and rolling, or rolling and manipulation. The equations of motion are derived in compact forms that embed an optimization criterion. These equations are used to obtain various useful forms of the robot kinematics. Using the developed modelling, actuation and control equations are derived that ensure the robot to track a desired path closely while maintaining balanced operations and tip-over avoidance. Various simulation results are provided for a hybrid rolling-walking robot traversing uneven terrain, which demonstrate the capabilities and effectiveness of the developed methodologies.

1 INTRODUCTION

Robots are becoming more sophisticated in mechanisms, control and intelligence to enable execution of complex tasks in challenging environments. In order to perform such tasks, various hybrid robots capable of multiple modes of operations such as combinations of rolling and walking, and rolling and manipulation as in mobile manipulators, have been proposed. In particular, hybrid locomotion of walking and rolling has received special attention. This is due to the fact that walking robots have superior performance for traversing uneven terrain. On the other hand rolling robots are better suited for relatively flat terrains as they can move faster and are more stable than walking robots in such terrain.

There are various methods to combine propulsion. Most mechanisms mount wheels at the end of legs that can be locked to act as feet. Robots that have been developed based on this mechanical architecture are usually four legged wheel-foot arrangements. These include Hylos (Grand et al, 2000), Paw (Smith et al, 2006), Primres-Sherpa (Cordes et al, 2011) and Workpartner (Ylonen and

Halme, 2002). The use of more than four legs adds to the complexity but also offers more versatility and extends application and behavioural diversity, such as stair climbing (Yuan and Hirose, 2004), high load carrying capability (Fujita and Sasaki, 2017), learning new locomotion when a leg is damaged (Cully et al, 2015; Jehanno et al 2014) and a highly articulated legged wheel-foot robot (Siegwart et al, 2002).

Kinematics analysis and motion control of wheeled robots and legged-foot robots have followed very different methodologies. The kinematic modelling of ordinary wheeled robots moving on flat surfaces was developed in (Muir and Neuman, 1991), and extended in (Rajagopalan, 1997), (Shin et al, 2001). The kinematics modelling of articulated rovers traversing uneven terrain poses a number of challenging problems that are much more complicated than the ordinary mobile robots moving over flat terrain. The first research work on kinematics modelling of an articulated wheeled robot over uneven terrain appears to be given in (Tarokh et al, 1999). In this work the kinematics of the Rocky 7 Mars rover is formulated. This work was subsequently generalized allowing modelling and analysis of rovers with active suspension systems (Tarokh and McDermott 2005), (Tarokh and McDermott, 2007) where three types of kinematics, namely navigation, actuation and slip kinematics, were identified and motion control was suggested.

^a  <https://orcid.org/0000-0002-1846-4570>

Subsequently, balance control and a recursive formulation of the kinematics for general articulated rovers were developed in (Tarokh et al, 2006), (Tarokh and Ho, 2013). More recently, (Kelly and Seegmiller, 2015) proposed a recursive formulation based on a differential algebraic formulation of the robot kinematics (Kelly, 2012)

There has been extensive work on motion planning of legged walking robots ranging from the mechanical considerations to foot placement, stability and gait optimization. A main consideration in walking robots is the stability and tip-over avoidance. Various techniques have been proposed, many based on the so called zero-moment-point (ZMP) and its modification (Winkler et al, 2017). An inverse kinematics is developed in (Shkolnik and Tedrake, 2007) for controlling the center of mass and the swing leg trajectory. A motion control of walking is proposed in (Zhong, 2016) using decentralized controller for a hexapod walking robot. Furthermore, (Winkler et al, 2018) proposes a trajectory optimization to determine gait sequence, foothold and swing leg motion. In order to achieve various dynamic gaits such as pace, trot and jumping (Bellicoseo et al, 2018) develops dynamic locomotion through nonlinear motion optimization.

The above mentioned papers and others propose variety of different methods for kinematics analysis and control, each applicable to a particular type of robot, i.e. rovers, walking robots, and mobile manipulators. However, there does not appear to exist a unified kinematics modelling and performance optimization that can be equally applied to hybrid robots with multiple modes of operations. In this paper we develop a unified kinematics modelling and control, incorporating optimization, for hybrid robots. Section 2 characterizes hybrid robots and various components needed for analysis, optimization and control. Section 3 develops kinematics modelling for hybrid robots. Optimization and control are discussed in Section 4. Simulation results for two modes of operation of a hybrid robot are provided in Section 5. Finally, Section 6 outlines the conclusions of the work.

2 CHARACTERIZATION OF GENERAL HYBRID ROBOTS

We define a general hybrid robot as the one with a body that is connected to a set of limbs, i.e. arms and legs. Each limb consists of a number of links and

joints which can be prismatic, revolute, or a combination of these. An arm is attached to a base and is terminated at an end-effector (hand) which is generally free to move in its workspace and can manipulate objects. On the other hand, a leg-end (wheel, foot, etc.) is generally in contact with the environment. A leg can be terminated at any one of the following: (i) a wheel for rolling on the terrain as in rovers and mobile robots, (ii) a foot that can be held on the terrain or lifted up and move as in walking robots, (iii) a wheel with a mechanism that can be locked so that it can act as a foot for walking or unlocked for rolling. This is the case for hybrid rolling and walking robots, (iv) a leg with simple or compound joints that connects a fixed base to a top platform and adjusts the position and orientation of the top platform by changing the leg length as in Stewart-type platforms.

A leg-end can be constrained, e.g. wheels of a rover or stance leg of a walking robot that are in contact with the terrain. It can also be free to move such as a swing leg of a walking robot.

A joint can be active (actuated) for adjusting its value, or be passive (compliant) for conforming to the environment, e.g. when a foot or a wheel touches the ground. For example space rovers, such as NASA Curiosity, use the so called rocker-bogie suspension system that has compliant (passive) joints to keep the rovers wheels in contact with the terrain when the robot mounts rocks. All six wheels of Curiosity are actuated (active), i.e. are independently steerable. As another example, a walking robot such as SILO4 (Gonzales, 2003) has three actuated joints and three compliant (passive) joints in each leg, as will be seen in Section 5. Usually all joints are sensed (measured).

For kinematics based control of a hybrid robot, we must develop models and formulate several techniques as follows:

- (a) An actuation kinematic model that relates the robot quantities to be controlled to the actuated joint variables. For example in a rover relating its pose (body position and orientation) rates to the wheel rolling and steering rates, and in a walking robot relating its body pose to the motion of the foot of the swing leg and joints angles of the both swing and stance legs.
- (b) A performance criterion whose optimization ensures a desirable operation of the robot, e.g. balancing a rover or a walking robot on a rough terrain to avoid tip-over. The optimization criterion can also include keeping the actuated joint angles close to the mid-values to avoid saturation of the joint actuators,

Using the above models, motion control enables the body pose and/or a foot/hand to follow desired trajectories while optimizing a certain performance criterion. It is noted that path planning and gait cycle are at a higher level than motion control, and in this paper we mainly concentrate on the latter assuming that a higher level planning is available.

3 KINEMATIC ANALYSIS AND MODELLING

The robots traversing rough terrain must move slowly, and for such slow motions kinematics modelling is sufficient. In this section we develop a kinematic formulation and modelling of hybrid robots. We also derive the fundamental kinematics equations a general hybrid robot.

We cascade a number of matrix transformations starting from the body reference frame B and terminating at a leg-end (foot, wheel, etc.) frame denoted by E_i , $i = 1, 2, \dots, \ell$ where ℓ is the number of legs with their ends in contact with the environment which contribute to the body movements.

The main body is connected to a leg through a set of linkages and joints, some of which are adjustable (active) using actuators and others can be passive (compliant). The linkages and joints connecting the body frame B to a leg-end is denoted by the $n_i \times 1$ joint variable vector q_i . There are a number of transformations between the body frame B and the leg-end frame E_i . We denote the overall cascaded transformation from the body B to a leg-end E_i by $T_{B,E_i}(q_i)$.

The transformation $T_{B,E_i}(q_i)$ does not reflect the motion, e.g. the motion of the legs-end and the resulting motion of the body frame. In order to describe these motions, we consider instantaneously coincident coordinates (ICC) frame (Muir, 1991) for the body denoted by \bar{B} . The ICC frame \bar{B} is coincident with B implying that $T_{\bar{B},B} = I_4$. However, the relative velocity between the two frames is not zero, i.e. $\dot{T}_{\bar{B},B} \neq 0$. When the body B moves with respect to the world coordinate system, a new ICC frame is assigned for each instant of time. The concept of ICC allows specifying the robot velocities independent of robot positions. We similarly define an ICC frame \bar{E}_i for the leg-end frame E_i for which $T_{\bar{E}_i,E_i} = I_4$ but the derivative $\dot{T}_{\bar{E}_i,E_i} \neq 0$. We can now cascade transformations and write

$$T_{\bar{B},B}(u_b) = T_{\bar{B},\bar{E}_i}(q_j) T_{\bar{E}_i,E_i}(u_{ei}) T_{E_i,B}(q_i) \quad (1)$$

$$i = 1, 2, \dots, \ell$$

where $u_b = (x_b \ y_b \ z_b \ \alpha_b \ \beta_b \ \gamma_b)^t = (p_b \ \varphi_b)^t$ is the 6×1 vector of the body pose consisting of the body position vector $p_b = (x_b \ y_b \ z_b)^t$ and the body orientation vector $\varphi_b = (\alpha_b \ \beta_b \ \gamma_b)^t$ where $\alpha_b, \beta_b, \gamma_b$ are roll, pitch and yaw respectively, and the superscript t denotes the transposition. Similarly $u_{ei} = (p_{ei} \ \varphi_{ei})^t$, $p_{ei} = (x_{ei} \ y_{ei} \ z_{ei})^t$ and $\varphi_{ei} = (\alpha_{ei} \ \beta_{ei} \ \gamma_{ei})^t$, $i = 1, 2, \dots, \ell$ are the pose, position and orientation vectors of the i -th leg-end, respectively

In order to describe motion, we take the derivative of (1) to get

$$\begin{aligned} \dot{T}_{\bar{B},B}(\dot{u}_b) &= \dot{T}_{\bar{B},\bar{E}_i}(\dot{q}_i) T_{\bar{E}_i,E_i}(u_{ei}) T_{E_i,B}(q_i) \\ &+ T_{\bar{B},\bar{E}_i}(q_i) \dot{T}_{\bar{E}_i,E_i}(\dot{u}_{ei}) T_{E_i,B}(q_i) \\ &+ T_{\bar{B},\bar{E}_i}(q_i) T_{\bar{E}_i,E_i}(u_{ei}) \dot{T}_{E_i,B}(\dot{q}_i) \end{aligned} \quad (2)$$

It is noted that $T_{\bar{B},\bar{E}_i}(q_j) = T_{B,E_i}(q_j)$ since the transformations relate two frames on the same robot, one with respect to the frame located on the moving robot and the other with respect with a world coordinate frame. In addition, while $\dot{T}_{\bar{B},\bar{E}_i}(\dot{q}_i) = 0$ due to the fact that \bar{B} and \bar{E}_i are instantaneous frames placed on the robot, the matrix $\dot{T}_{B,E_i}(\dot{q}_i) \neq 0$ since it relates the transformation derivative with respect to the world coordinates which changes with the robot motion. In addition $T_{\bar{E}_i,E_i}(u_{ei}) = I_4$. Bearing in mind the above properties, (2) reduces to the following which we refer to as the *fundamental kinematics equation* of a hybrid robot.

$$\begin{aligned} \dot{T}_{\bar{B},B}(\dot{u}_b) &= T_{B,E_i}(q_i) \left(\dot{T}_{\bar{E}_i,E_i}(\dot{u}_{ei}) T_{E_i,B}(q_i) \right. \\ &\quad \left. + \dot{T}_{E_i,B}(\dot{q}_i) \right) \\ &i = 1, 2, \dots, \ell \end{aligned} \quad (3)$$

Equation (3) describes the motion of the robot body in terms of the motions of the leg-ends as well as joint angle rates. The transformation matrix $T_{B,E_i}(q_i)$ is computed using the Denavit-Hartenberg (D-H) table connecting the body to a leg end.

Since $\dot{T}_{\bar{B},B}(u_b)$ in (3) describes the motion of a general body, it can also be expressed as

$$\dot{T}_{\bar{B},B}(\dot{u}_b) = \begin{pmatrix} 0 & -\dot{\gamma}_b & \dot{\beta}_b & \dot{x}_b \\ \dot{\gamma}_b & 0 & -\dot{\alpha}_b & \dot{y}_b \\ -\dot{\beta}_b & \dot{\alpha}_b & 0 & \dot{z}_b \\ 0 & 0 & 0 & 0 \end{pmatrix} \quad (4)$$

Note that the upper left 3×3 submatrix in (4) is skew symmetric and its last row is a zero vector. It is noted that the two terms in the right hand sides of (3) have the same structure as (4), i.e. their upper left 3×3 submatrices are skew symmetric and the last

row is a 0 vector, and this statement can be proven mathematically.

It is evident that the left hand side of (3) contains the components of the body pose vector rate \dot{u}_b while its right hand side is functions of the leg-ends pose rate \dot{u}_{ei} and joint angle vector q_i as well as its rate \dot{q}_i . We substitute into (3) the body and leg-end motion transformation $T_{\bar{B},B}(\dot{u}_b)$ using (4). Similarly, $T_{\bar{E}i,Ei}(\dot{u}_{ei})$ can be expressed in the form of (4) by replacing the subscripts \bar{B},B with $\bar{E}i,Ei$ and the subscript b with ei , respectively. We then set equal the like terms on both sides of acquired equation. This will enable us to write (3) as

$$\dot{u}_b = F_i(q_i) \dot{u}_{ei} + G_i(q_i) \dot{q}_i ; i = 1, 2, \dots, \ell \quad (5)$$

where $F_i(q_i)$ and $G_i(q_i)$ are respectively 6×6 and $6 \times n_i$ matrices. Equation (5) describes the contribution of individual leg-end motions and joints in each leg to the robot body motion. The net body motion is the composite effect of all legs which is obtained by combining (5) into a single matrix equation as

$$I \dot{u}_b = F(q) \dot{u}_e + G(q) \dot{q} \quad (6)$$

where $I = (I_6 \dots I_6)^t$, I_6 is the 6×6 identity matrix, I is a $6\ell \times 6$ matrix, $\dot{u}_e = (\dot{u}_{e1} \dots \dot{u}_{e\ell})^t$ is the $6\ell \times 1$ composite vector of leg-end pose rates, and $\dot{q} = (\dot{q}_1 \dots \dot{q}_\ell)^t$ is the composite $n_q \times 1$ vector of joint angle velocities. The robot composite matrices $F = \text{blockdiag}(F_1(q_1) \dots F_\ell(q_\ell))$ and $G = \text{blockdiag}(G_1(q_1) \dots G_\ell(q_\ell))$ are $6\ell \times 6\ell$ and $6\ell \times n_q$, respectively. It is noted from (6) that we can determine the robot body motion given the motion of the leg-ends, and joints velocities.

For some cases, i.e. a manipulator attached to a mobile body, it is convenient to express the limb-end (arm-end) motion in terms of base/body motion and joint velocities. In this case using a development similar to that leading to (3), we find

$$\begin{aligned} T_{\bar{E}i,Ei}(\dot{u}_{ei}) &= T_{Ei,B}(q_i) \left(T_{\bar{B},B}(\dot{u}_b) T_{B,Ei}(q_i) \right. \\ &\quad \left. + T_{B,Ej}(\dot{q}_i) \right) \end{aligned} \quad (7)$$

$$i = 1, 2, \dots, \ell$$

Equation (3) and (7) are the *companion forms*. Equation (7) is of the same form as (3) and thus the developments leading to (6) can be applied to (7) to get

$$\dot{u}_e = H(q) I \dot{u}_b + J(q) \dot{q} \quad (8)$$

where I and \dot{u}_e are as defined as before and $H(q)$ and $J(q)$ are $6\ell \times 6\ell$ and $6\ell \times n_q$ matrices, respectively. We refer to (8) as *limb-end kinematics*.

Equations (8) is used when the motion of the limb-ends must be determined for a given body motion. In addition equation (8) can be used for situations where one or more arms are attached to the robot body and the motion of the arm-ends (end-effectors) are needed in term of the motion of the robot body \dot{u}_b and the arm joint velocities. This is the case of a mobile manipulator, a manipulator attached to a walking robot or to a Stewart-like parallel manipulator. In such cases, the body motion, which is the results of legs ends (wheels or feet) motions, is obtained using (6). The arms ends motions are then found using an equation of the form (8), i.e.

$$\dot{u}_{ak} = H_k(q_k) I \dot{u}_b + J_k(q_k) \dot{q}_k ; k = 1, 2, \dots, m \quad (9)$$

where \dot{u}_{ak} is the arm end motion, q_k an arm joints angle vector, and m is the number of arms. If an arm base is attached to the robot body at the body reference frame $H_k(q_k) = I_6$.

We have developed a program in Matlab that takes the D-H table of a robot with ℓ legs and m arms with n_i , $i = 1, 2, \dots, \ell$ joints in each leg and n_k , $k = 1, 2, \dots, m$ joints in each arm, and performs symbolic manipulation to obtain the equations of motion in the forms of (6), (8) and (9).

The purpose of motion control is to determine the actuated joint values so that the body or leg-ends follow the desired trajectories while achieving certain desired characteristics. For rovers and walking robots moving on uneven terrains such characteristics can be balancing to avoid tip over, and for manipulators and parallel robots it can be, for example, minimum joint angle changes.

4 OPTIMIZATION AND CONTROL

The main goal of optimization is to keep the robot balanced to avoid tip over when traversing rough terrain. A further optimization objective is to operate the joints as close to their center values so as to prevent joint limits. The main goal of control is to keep the rover on the desired path.

For the purpose of optimization and control, we consider (6) and identify four set of quantities among components of body pose rate \dot{u}_b , leg-end pose rate \dot{u}_e and joint rate \dot{q} as follows.

Actuated quantities: These are adjustable components of the joint vector \dot{q} , denoted by $n_a \times 1$ vector $\dot{X}_{act} \subset \dot{q}$ which can be adjusted (controlled).
Unknown quantities: These are quantities that are unmeasurable and unknown. Example of these

quantities are leg-end (e, g. wheel) side slip which is a component of \dot{u}_e . These are denoted by the $n_u \times 1$ vector $\dot{X}_{unk} \subset \dot{u}_e$.

Desired Quantities: These are the quantities that are specified and must be controlled. Examples of such quantities are the desired trajectories of the rover body (\dot{x}_b, \dot{y}_b) or leg-end (foot) in the case of walking to follow a path. These quantities are represented by the $n_d \times 1$ vector $\dot{Y}_{des} \subset (\dot{u}_b, \dot{u}_e)$.

Known quantities: These include measured roll and pitch rates of the body $\dot{\alpha}_b$ and $\dot{\beta}_b$ as well as compliant joint values. In addition some quantities such as wheel sway slip $\dot{\alpha}_e$ and tilt slip $\dot{\beta}_e$ may be zero due to the mechanical design of the wheel attachment to the leg. The known quantities are denoted by the $n_k \times 1$ vector $\dot{Y}_{kno} \subset (\dot{q}, \dot{u}_b, \dot{u}_e)$.

Using the above characterization of the quantities, we partition and rearrange (6) as

$$(\mathcal{A}_1 \quad \mathcal{A}_2) \begin{pmatrix} \dot{X}_{act} \\ \dot{X}_{unk} \end{pmatrix} = (\mathcal{B}_1 \quad \mathcal{B}_2) \begin{pmatrix} \dot{Y}_{des} \\ \dot{Y}_{kno} \end{pmatrix} \quad (10)$$

where \mathcal{A}_1 , \mathcal{A}_2 , \mathcal{B}_1 and \mathcal{B}_2 are obtained from $I, F(q)$ and $G(q)$ as a result of partitioning (6). The above equation must be solved to find the values of actuated joint angles \dot{X}_{act} and unknown quantities \dot{X}_{unk} . Equation (10) is of the form

$$\mathcal{A}\dot{X} = \mathcal{B}\dot{Y} \quad (11)$$

where X and Y are, respectively, the unknown and known vectors of dimensions $(n_a + n_u) \times 1$ and $(n_d + n_k) \times 1$ and \mathcal{A} and \mathcal{B} are $6\ell \times (n_a + n_u)$ and $6\ell \times (n_d + n_k)$ matrices, respectively. The existence, uniqueness or multiple solutions for the unknown vector X in (11) is determined by $rank(\mathcal{A} \mathcal{B})$. In general most rovers, walking robots, mobile manipulators, parallel manipulators, and redundant arms have more actuated joints and unknown quantities than the number of known/desired quantities. In other words, in general (11) is an underdetermined systems of equations and there are infinite number of solutions to (11). The general solution to (11) is of the form

$$\dot{X} = \mathcal{A}^\# \mathcal{B} \dot{Y} + c(I_{6\ell} - \mathcal{A}^\# \mathcal{A}) \Gamma(X) \quad (12)$$

where $\mathcal{A}^\#$ is the pseudo-inverse of \mathcal{A} , c is a constant scalar, $I_{6\ell}$ is an identity matrix of dimension $6\ell \times 6\ell$, and $\Gamma(X)$ is an arbitrary free vector of size $6\ell \times 1$. The free vector $\Gamma(X)$ can be used for the optimization of a performance index function $f(X)$ if we set (Nakamura, 1991)

$$\Gamma(X) = \frac{\partial f(X)}{\partial X}$$

The vector X consists of actuated joints X_{act} and unknown quantities X_{unk} . However, only X_{act} is adjustable and is the independent variable; the other component, i.e. vector X_{unk} , is dependent. As a result the free vector $\Gamma(X)$ is set to

$$\Gamma(X) = \begin{pmatrix} \frac{\partial f(X)}{\partial X_{act}} \\ 0 \end{pmatrix} \quad (13)$$

where $\partial f(X)/\partial X_{act}$ is an $n_a \times 1$ vector, and 0 is the zero vector of size $(6\ell - n_a) \times 1$. The performance index function to be minimized can be a variety of forms for different robots and objectives.

The freedom is brought about by the extra actuators that usually exist in an active suspension system. We will use this freedom to balance the robot configuration as it moves over rough terrain. In such terrain with many bumps and dips, without balance control, the rover can lose balance and can tip over. We must now define and quantify more precisely the notion of a balanced configuration and express it in terms of the rover center of mass and adjustable joint angles. Stability measures for quasi-static situation, i.e. when the robot moves slowly, have been suggested before, e.g. (Iagnemma, 2000). Here, we use a somewhat different formulation. Suppose we draw a vector from the center of mass (CoM) to each leg end-terrain contact position p_{ei} and denote the unit vector by v_i . Each consecutive pair of such unit vectors, i.e. v_i and v_{i+1} form a plane denoted by π_i . The unit vector perpendicular (normal) to this plane is given by

$$w_i = v_i \times v_{i+1}; i = 1, 2, \dots, \ell \quad (14)$$

where $v_{n+1} \equiv v_1$. The unit gravity vector g can be expressed in terms of body roll and pitch angles as

$$g = (\sin \beta_b \quad -\sin \alpha_b \cos \beta_b \quad \cos \alpha_b \cos \beta_b)^t \quad (15)$$

Now consider the dot product between unit vectors w_i and g , i.e.

$$\lambda_i = g^t \cdot w_i \quad (16)$$

When the gravity vector g lies in any of the plane π_i , the vectors g and w_i become orthogonal, resulting in $\lambda_i = 0$ and the robot becomes on the verge of tipping over. On the other hand, when the vectors g and w_i are along the same direction $\lambda_i = 1$, $i = 1, 2, \dots, \ell$; the robot is in the most stable configuration. We define the tip over measure Λ_{to} as the aggregate of all λ_i , i.e. $\Lambda_{to} = (1 - \prod_{i=1}^{\ell} \lambda_i)$. Higher values of Λ_{to} correspond to higher possibility of tip over. It is noted that for a walking robot when one or more legs are not in contact with

the terrain the number of leg end contact points reduces by the number of swing legs. For example for a quadruped there are three contact points when a leg is off the ground, and the center of mass must be such that $\Lambda_{t_0} > 0$ at each instant of time. This amounts to the projection of the center of mass on the terrain to be inside the triangle formed by the three stance feet (leg-ends).

We now define the optimization (minimization) function $f(\mathcal{X})$ in (12) as

$$f(\mathcal{X}) = k_{t_0} \Lambda_{t_0} + \Delta \mathcal{X}_{ac}^t K_{act} \Delta \mathcal{X}_{act} \quad (17)$$

The first in (14) with the scalar weighting k_{t_0} is used to avoid tip-over of the robot. The second term with $\Delta \mathcal{X}_{act} = (\mathcal{X}_{act} - \bar{\mathcal{X}}_{act})$ ensures that the actuated joint angles \mathcal{X}_{act} operate close to their middle values $\bar{\mathcal{X}}_{act}$ so as to avoid joints taking extreme values which can result in a maximally flat robot e.g. legs stretched outwards, or saturation of the joints, i.e. jointing hitting their limits. The matrix K_{act} can be chosen as a constant diagonal matrix. For redundant manipulators and parallel robots, the performance index can be the minimum joint angle changes, in which case k_{t_0} is set to zero.

Equation (12) finds the values of the actuated joints \mathcal{X}_{act} to obtain the desired quantities \mathcal{Y}_{des} in an open-loop fashion, and thus does not guarantee zero or small error between the actual (measured) and desired values. Therefore, we apply a control law using the error between the desired \mathcal{Y}_{des} and its actual (measured) value \mathcal{Y}_{msd}

$$\mathcal{E} = \mathcal{Y}_{des} - \mathcal{Y}_{msd} \quad (18)$$

The control consists of two steps. In the first step at time $(t-1)$ we find an estimate of the unknown vector $\dot{\mathcal{X}}_{unk}(t-1)$ from (12) by premultiplying both sides of this equation by \mathcal{A} which results in $\mathcal{A}(I_{6\ell} - \mathcal{A}^\# \mathcal{A}) = 0$, and together with (10) gives

$$\begin{aligned} \mathcal{A}_2 \dot{\mathcal{X}}_{unk}(t-1) = \\ \mathcal{B}_1 \dot{\mathcal{Y}}_{des}(t-1) + \mathcal{B}_2 \dot{\mathcal{Y}}_{kno}(t-1) - \mathcal{A}_1 \dot{\mathcal{X}}_{act}(t-1) \end{aligned} \quad (19)$$

In the next time sample (t) we use the acquired $\dot{\mathcal{X}}_{unk}(t-1)$ for controlling the actuated joints in the control law

$$\begin{aligned} \dot{\mathcal{X}}_{act}(t) \\ = \mathcal{A}_1^\# \{ \mathcal{B}_1 \dot{\mathcal{Y}}_{msd}(t) - \kappa \mathcal{B}_1 \mathcal{E}(t) + \mathcal{B}_2 \dot{\mathcal{Y}}_{kno}(t) - \mathcal{A}_2 \dot{\mathcal{X}}_{unk}(t-1) \} \end{aligned} \quad (20)$$

where κ is a scalar controller gain. Note that all quantities in the right hand side of (20) are known. We refer to (20) as *optimized actuation kinematics*. Note that (20) is in effect a proportional plus integral

(PI) control for \mathcal{X}_{act} . Substituting (18) into (20) and simplifying we get

$$\dot{\mathcal{E}}(t) = -\kappa \mathcal{E}(t) + \mathcal{B}_1^\# \mathcal{A}_2 \delta \quad (21)$$

where $\delta = \dot{\mathcal{X}}_{unk}(t) - \dot{\mathcal{X}}_{unk}(t-1)$ is small for small sample time. Provided that \mathcal{B}_1 is not ill-conditioned, the solution to (21) is

$$\mathcal{E}(t) = e^{-\kappa t} + \frac{1}{\kappa} \mathcal{B}_1^\# \mathcal{A}_2 \delta \quad (22)$$

Equation (22) implies that the error decreases exponentially to a small value if the gain κ is chosen to be relatively large.

5 SIMULATION STUDIES OF A HYBRID ROBOT

In this section we discuss the implementation of a hybrid rolling and walking robot where the rolling takes place in a relatively smooth terrain and is transformed to walking when the robot faces uneven terrains.



Figure 1: A leg of SILO4 walking robot (Gonzales et al, 2003) showing its various active and passive joints.

We will apply our kinematics modeling and control to SILO4 (Gonzales, 2003) which is a walking robot shown in Fig. 1. SILO4 is a versatile quadruped walking robot that has four identical legs. Each leg has a shoulder joint, a hip and a knee joint that are actuated. In addition, it has three passive (compliant) joints, i.e. ankle, heel and sole that conform to the terrain during walking. To make the robot hybrid, we attach wheels at the leg ends, as depicted in Fig. 2. During walking, wheels are locked and act as feet. In the rolling mode, the conforming foot joints are locked and the wheels are free to rotate.

In addition due to mechanical design of SILO4 that is intended for walking rather than hybrid operation, in the rolling mode the steering is performed through the shoulder joint angle rather than at the wheel. This makes control and path following challenging.

The four vectors mentioned in Section 4, namely, desired \dot{Y}_{des} , actuated \dot{X}_{act} , known \dot{Y}_{kno} and unknown \dot{X}_{unk} that are used for optimization and control are specified below for rolling and walking of this robot.

Rolling: In this mode the desired quantities are the trajectories of the rover body velocities which must follow a desired path on the terrain, and thus $\dot{Y}_{des}(t) = (\dot{x}_b(t) \dot{y}_b(t))^t$. The known quantity vector \dot{Y}_{kno} consists of wheel linear velocities which are obtained by transforming $(\dot{x}_b(t) \dot{y}_b(t))^t$ to the wheel velocities \dot{x}_i and \dot{y}_i , $i = 1,2,3,4$ so as to roll the wheels along the desired rover body trajectory. Note that $\dot{x}_i = r \dot{\theta}_i$ where r is the wheel radius and $\dot{\theta}_i$ are the wheels angular velocities. Since the wheels are constrained to be on the terrain, z_i is also known from the terrain topology. We assume sensors such as laser ranger finders or cameras are available to map the terrain elevations in front of the robot. In addition due to the mechanical constraints, wheel roll rate $\dot{\alpha}_i = 0$. The wheel pitch rate $\dot{\beta}_i$ is determined by the terrain inclination under the wheel and is therefore known. Finally the wheel yaw rate $\dot{\gamma}_i$ is known since it must follow the desired wheel trajectory. The actuated quantity vector \dot{X}_{act} consists of the three leg joint angles in each of the four legs \dot{q}_{ij} , $i = 1,2,3,4$; $j = 1,2,3$. The unknown quantity vector \dot{X}_{unk} comprises of the body roll, pitch and yaw rates $\dot{\alpha}_b, \dot{\beta}_b, \dot{\gamma}_b$ respectively, and the body vertical movement \dot{z}_b .

Walking: We assume that a planner is available that determines the sequence of leg movements (gait cycle). In the simulations, we use the following sequence of leg movements: left front leg, right back leg, right front leg, left back leg. In the above wheel rolling, we specified the velocity trajectories of the body $(\dot{x}_b(t) \dot{y}_b(t))^t$ and the wheels follow these specifications through the transformations from the body to the wheels, making the body the leader and the wheels followers. In walking, we specify the trajectories of the swing leg and the body is to follow the leg movement, i.e. the swing leg is the leader and the body is the follower. We specify a semi-circle path for the foot of the swing leg between its current position on the terrain and the next point on the desired path based on the terrain topology in front of the robot. As mentioned before, path planning is not the thrust of this paper. During walking the three passive foot joints are unlocked and become compliant (unknown). In addition the stance feet

velocities $\dot{x}_i = \dot{y}_i = \dot{z}_i = 0$ since these feet must be fixed on the terrain.

The transition between walking and rolling takes place using body roll α_b and pitch β_b . The transition from rolling to walking takes place when $(\alpha_b^2 + \beta_b^2) > a + \epsilon$, and from walking to rolling when at the time when the four feet touch the ground and $(\alpha_b^2 + \beta_b^2) < a - \epsilon$ where a is a threshold and 2ϵ is the hysteresis width used to avoid oscillating between rolling and walking. Alternatively a laser ranger finder or cameras can determine the terrain topology and decide the transition.

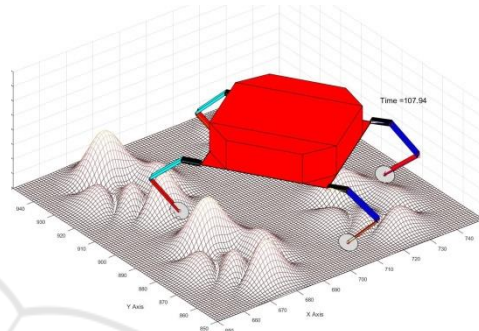


Figure 2: Robot on a small section of the terrain.

In order to test the performance of the kinematic modeling and control, we consider a terrain which has both bumps and relatively flat surfaces a small section of which is given in given in Fig. 2. The maximum height of bumps is 20 cm. The desired path is chosen to be circular with a radius of about $r = 2.5$ meters which the robot traverses in about 400 seconds, giving the average linear speed of 2.35 m/s which is equal to fast human walk. The desired circle defines two other circles with radii $r - \frac{b}{2}$ and $r + \frac{b}{2}$ where b is the width of the rover. One side of the rovers wheels/feet is desired to traverse over the inner blue circle in Fig. 3, and the other side is specified traverse on the outer green circle.

The optimization criterion (17) is applied with $k_{to} = 1$ and $K_{act} = I$ to keep the rover balanced and maintain the legs joints with angles close to their center ranges.

The variations of the three actuated joint angles of leg 2 are given in Fig. 4 for one full cycle, i.e. during the time when all four legs complete their motion which takes about 3.5 second. The joint angles variations in the other legs, not shown due to space limitation, exhibit similar responses. Fig. 5 shows the traces of the body, links and joint, and feet (locked wheels) for one cycle of walking after all four feet have gone through their semi-circle paths. Note that at any time

only the swing foot is moved and the other three stance feet are stationary.

In Fig. 6 we show the joint angles in another leg, namely leg 4, during the traversal of the whole circular path which takes about 400 s. Note that significant changes of joints angles take place during walking when the robot traverses over bumps. This is necessary to keep the rover balanced as one leg is lifted from the ground and the body moves forward. The periods of low angle variations in Fig. 6 are due to wheels rolling, rather than walking, over the relatively smooth part of the terrain.

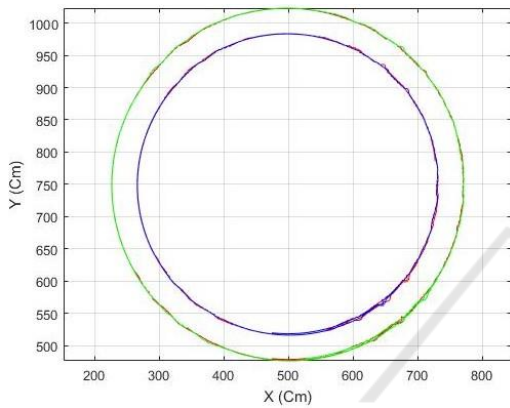


Figure 3: The desired inner side (in blue) and outer side (green) of the paths for the wheels/feet. The actual paths are shown in red.

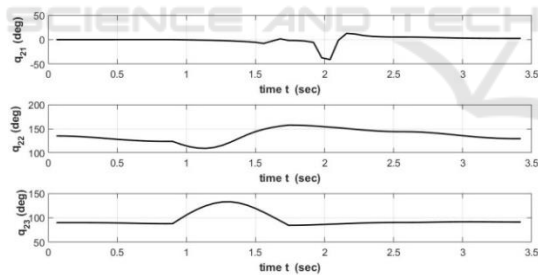


Figure 4: The variations of joints of leg 2 during one cycle of walk.

The rover balance as reflected in the body pitch and roll is provided in Fig. 7. It is seen that the optimization (17) has kept the robot pitch and roll small, with the maximum roll of about 10 degrees and the maximum pitch of 5 degrees, essentially levelling the robot despite variations in the terrain topology.

The traces of the desired circular paths of the inner and outer wheels/feet are shown in Fig. 3, in green and blue, respectively, and actual paths traversed by the robot wheel and feet are shown on both circles in red. It is evident that the control scheme described in Section 4 has kept the robot very close to the desired

path with a maximum error of about 5 cm.

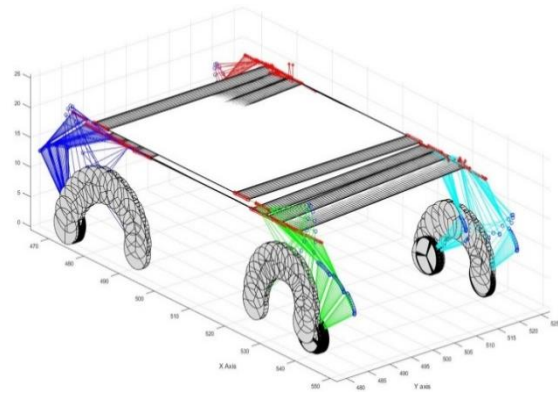


Figure 5: The traces of feet (locked wheels) for one cycle after all feet have completed their trajectories.

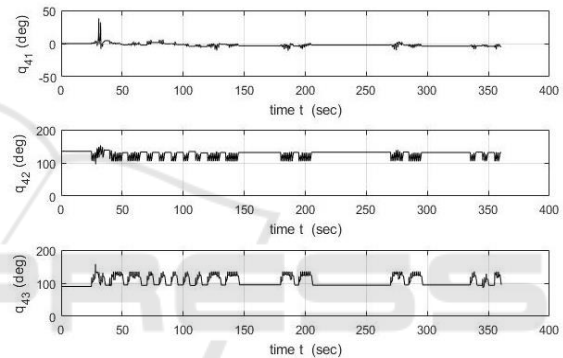


Figure 6: Leg 4 joints angles variation during the whole period of traversing the circular path.

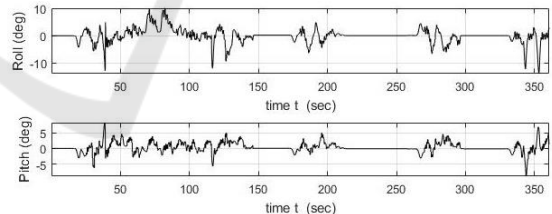


Figure 7: Body pitch and roll variation during traversal of the circular path.

6 CONCLUSIONS

Traditional approaches to kinematics modelling, optimization and control of robots have used a variety of different methods each suitable for a particular type of robot. In contrast this paper has developed a unified kinematics modelling with an embedded optimization criterion in a form which can be applied to almost any type of robot. The fundamental kinematics equation of a general hybrid robot is

presented in a compact form. This equation is then used to derive the kinematics equations in several useful forms such as companion, actuation, optimization and control forms. The proposed unified approach can be applied to various robots, including any combination of propulsion such as hybrid walking/rolling, mobile manipulators and Stewart-type platforms. A software package has been developed to implement the kinematics modelling and optimization in its various forms. The software includes animation of the robot motion. The program has been applied to a hybrid walking/rolling robot for traversing on bumpy terrain. Various results demonstrate the satisfactory performance of the systems in path following, balancing and tip-over avoidance.

REFERENCES

- Bellicoseo, C.D., Jenelten, F., Gehring, C. and Hutter, M., 2018. Dynamic locomotion through online nonlinear motion optimization for quadruped robots," *IEEE Robotics and Automation Letters*, vol. 3, no. 3, pp. 2261-2268.
- Cordes, F., Dettmann, A., and Kirchner, A., 2011. Locomotion modes for a hybrid wheeled-legplanetary rover, in *Proc. of IEEE Int. Conf. on Robotics and Biomimetics*, vol. 1, pp. 654-659, 2004.
- Cully, A., Clune, J., Tarapore, D., and Mouret, J-B., 2015. Robots that can adapt like animals," *Nature* volume 521, pp. 503-507.
- Gonzales de Santos, P., Estremera, J., and Garcia, E., 2003. "The SILO4- A true walking robot for comparative study of walking machines techniques. *IEEE Robot. Autom. Mag.*, vol. 10, no. 4, pp. 23- 32.
- Grand, C. BenAmar, F., Plumet, F. and Bidaud, P., 2000. Stability control of a wheel-legged mini-rover, in *Proc of Int. Conf. on Climbing and Walking Robots*.
- Fujita, T., and Sasaki, T., 2017. "Development of hexapod tracked mobile robot and its hybrid locomotion with object-carrying." *IEEE Int. Symp. on Robotics and Intelligent Sensors*.
- Iagnemma, K., Rzepniewski, A., Dubowsky, S., Huntsberger, T., Pirjanian, P., Schenker, P., 2000. Mobile Robot Kinematic Reconfigurability for Rough-Terrain," *Proceedings of the SPIE Symposium on Sensor Fusion and Decentralized Control in Robotic Systems III*.
- Jehanno, J-M., Cully, A., Grand, C., and Mouret, J-B., 2014. "Design of a wheel-legged hexapod robot for creative adaptation," *World Scientific Publishing*, vol. 20, no. 6.
- Kelly, A. and Seegmiller, N. 2015 "Recursive Kinematic Propagation for Wheeled Mobile Robots", vol. 34, no. 3, *Int. J. Robotics Research*.
- Kelly, A., 2012 "A vector algebra formulation of mobile robot velocity kinematics," *Proc. 2012 Int. Conf. Field and Service Robots*.
- Muir, P.F., and Neuman, C. P., 1991. "Kinematic modeling of wheeled mobile robots," *J. Robotic Systems* vol. 4, no. 2, pp. 281-340.
- Nakamura, N., 1991. *Advanced Robotics-Redundancy and Optimization*, Chapter 4, Addison-Wesley.
- Rajagopalan, R., 1997 "A generic kinematic formulation for wheeled mobile robots," *Journal of Robotic Systems* vol. 14, no. 2, pp. 77-91.
- Shkolnik, A. and Tedrake, R. 2007. "Inverse Kinematics for a Point-Foot Quadruped Robot with Dynamic Redundancy Resolution", 2007 *IEEE Int. Conf. Robotics and Automation* Roma, Italy.
- Siegwart, R., Lamon, P., Estier, T., Lauria, M., and Piguet, R., 2002. "Innovative design for wheeled locomotion in rough terrain," *Robotics and Autonomous Systems*, vo. 40, pp. 151-162.
- Shin, D.D., and K.H. Park, K.H., 2001. "Velocity kinematic modeling for wheeled mobile robots," *Proc. 2001 IEEE Int. Conf. Robotics and Automation*, vol. 4, pp. 3516-3522.
- Smith, J., Sharf, I., and M. Trentini, M., 2006. Paw: a Hybrid wheeled-leg robot, in *Proc. of IEEE Int. Conf. on Robotics and Automation*.
- Tarokh, M., McDermott, G., Hayati, S., and Hung, J., 1999 "Kinematic modeling of a high mobility Mars rover," *Proc. IEEE Int. Conf. Robotics and Automation*, pp. 992-998.
- Tarokh, M. and McDermott, G., 2005. Kinematics modelling and analysis of articulated rovers. *IEEE Trans. Robotics*, vol. 21, no. 4, pp. 439-454.
- Tarokh, M., G. McDermott and L. Mireles, 2006. Balance control of articulated rovers with active Suspension. *Proc. 8th IFAC-IEEE Symposium on Robot Control: Vol. FrP- 2.1-2*, pp. 1-6. Bologna, Italy.
- Tarokh, M., and McDermott, G., 2007. "A systematic approach to kinematics modeling of high mobility wheeled rovers," *Proc. IEEE Int. Conf. Robotics and Automation*, pp. 4905- 4910, Rome, Italy.
- Tarokh, M., Ho, H.D., and A. Bouloubasis, A., 2013. Systematic kinematics analysis and balance control of high mobility rovers over rough terrain," *J. Robotics and Autonomous Systems*, 61, 13-24.
- Winkler, A.W., Farshidian, F., Pardo, D., Neunert, M., and Buchli, J., 2017. "Fast Trajectory Optimization for Legged Robots Using Vertex-Based ZMP Constraints," *IEEE Robotics and Automation Letters*, Vol. 2, No. 4, pp.2201-2208.
- Winkler, A.W., Bellicoso, C.D., Hutter, M. and J. Buchli, J., 2018. "Gait and trajectory optimization for legged systems through phased-based end-effector parameterization," *IEEE Robotics and Automation Letters*, vol.3, no. 3, pp. 1560-1567.
- Ylonen, S., and Halme, A., 2002. Further development and testing of the hybrid locomotion of Workpartner robot, in *Proc of Int. Conf. on Climbing on Walking Robots (CLAWAR)*.
- Yuan, J., and S. Hirose, S., 2004. "Research on leg-wheel hybrid stair- climbing robot,zero carrier," in *IEEE Int. Conf. on Robotics and Biomimetics*.

Zhong, G., Deng, H., Xin, G., and Wang, G., 2016. Dynamic Hybrid Control of a Hexapod Walking Robot: Experimental Verification,” IEEE Trans. Industrial Electronics, , Vol. 63, No. 8. pp.5001-5011.

